

LABORATORY ANALYSIS OF PRESOLAR SILICATE STARDUST FROM A NOVA

J. LEITNER^{1,4}, J. KODOLÁNYI^{1,2}, P. HOPPE¹, AND C. FLOSS³

¹ Max Planck Institute for Chemistry, Particle Chemistry Department, Hahn-Meitner-Weg 1, D-55128 Mainz, Germany; jan.leitner@mpic.de

² Department of Geology and Soil Science, Ghent University, Krijgslaan 281 S8, B-9000 Gent, Belgium

³ Laboratory for Space Sciences and Physics Department, Washington University, One Brookings Drive, St. Louis, MO 63130, USA

Received 2012 May 17; accepted 2012 July 5; published 2012 July 18

ABSTRACT

We report the major element as well as the oxygen, magnesium, and silicon isotope composition of a unique presolar silicate grain found in the fine-grained fraction of the Antarctic CR2 chondrite Graves Nunataks 95229. The grain is characterized by an extremely high $^{17}\text{O}/^{16}\text{O}$ ratio ($6.3 \pm 0.2 \times 10^{-3}$) relative to solar values, whereas its $^{18}\text{O}/^{16}\text{O}$ ratio is solar within measurement uncertainty. It also shows enrichments in $^{25,26}\text{Mg}$ and a significant excess in ^{30}Si relative to solar system compositions, with $\delta^{25}\text{Mg} = 79 \pm 21\%$, $\delta^{26}\text{Mg} = 70 \pm 20\%$, and $\delta^{30}\text{Si} = 379 \pm 92\%$. This isotopic composition is consistent with an origin in the ejecta of a $\sim 1.3\text{--}1.4 M_{\odot}$ ONe nova with large contributions of material from a main-sequence companion star of roughly solar metallicity. However, many details of the stellar source remain undetermined, owing to the uncertainties of current nova nucleosynthesis models. Auger electron spectroscopic analyses identify O, Mg, Si, and Fe as the grain's major constituents. Its $(\text{Mg} + \text{Fe})/\text{Si}$ atomic ratios are lower than that of olivine and correspond on average to Fe–Mg–pyroxene. A complex texture and heterogeneous major element distribution within the grain attest to condensation under non-equilibrium conditions, which is consistent with the proposed nova origin.

Key words: astrochemistry – circumstellar matter – novae, cataclysmic variables – nuclear reactions, nucleosynthesis, abundances – stars: winds, outflows

Online-only material: color figures

1. INTRODUCTION

Refractory dust grains with highly anomalous isotopic compositions are found in small quantities in primitive meteorites, interplanetary dust particles, and cometary matter (e.g., Zinner 2007; Hoppe 2008). These “presolar” grains have formed in the winds of evolved stars or in the ejecta of stellar explosions. After passage through the interstellar medium (ISM), they were incorporated in the dust and gas cloud from which our solar system formed ~ 4.6 Ga ago. A fraction of them survived alteration and homogenization processes during solar system formation and represent samples of ancient stardust available for laboratory analyses. Investigation of their isotopic compositions and mineralogy provides valuable information on stellar nucleosynthesis and evolution, grain growth in circumstellar environments, types of stars that contributed material to the protosolar molecular cloud, and chemical and physical processes in the ISM.

Refractory silicates and oxides are among the most abundant presolar grain types. Most ($>99\%$) of these grains are divided into four distinct groups, according to their oxygen isotopic compositions (Nittler et al. 1997, 2008; Nguyen et al. 2007). Group 1–3 grains ($\sim 90\%$) come from low-mass ($1.2\text{--}2.2 M_{\odot}$) asymptotic giant branch (AGB) stars, whereas grains of Group 4 ($\sim 10\%$) most likely formed in the ejecta of Type II supernovae (SNeII; Nittler et al. 2008; Vollmer et al. 2008). Another small fraction ($\leq 1\%$) displays $^{17}\text{O}/^{16}\text{O}$ ratios ($>5\text{--}6 \times 10^{-3}$) that cannot be produced in single AGB stars (Nittler et al. 2008; Gyngard et al. 2011; Palmerini et al. 2011). These “extreme Group 1” grains are believed to stem from binary star systems with mass transfer (Nittler et al. 2008); some of them might have formed in the ejecta of nova explosions (Nittler & Hoppe 2005; Nittler et al. 2008, 2012; Gyngard et al. 2010, 2011).

Classical novae are stellar explosions that occur in close binary star systems, where a white dwarf (WD) star accretes hydrogen-rich material from a nearby companion, typically a K or M main-sequence star of solar composition. Sustained mass accretion from the companion star increases the envelope temperature up to a few 10^8 K. The ensuing thermonuclear runaway triggers the nova outburst. Depending on white dwarf composition and mass, nova outbursts are divided into CO- (WD composed mainly of C and O, $M_{\text{WD}} < 1.1 M_{\odot}$) and ONe-novae (WD composed of O, Ne, and some Mg; $M_{\text{WD}} \geq 1.1 M_{\odot}$).

Infrared and ultraviolet observations (e.g., Gehrz et al. 1998; Shore et al. 1994) suggest that novae form grains in their expanding ejecta. While frequent dust formation is observed around CO novae, ONe novae are not such prolific dust producers. Their ejecta have lower masses and higher expansion velocities than those of CO novae, and the typical local densities in the expanding shells may be too low to allow significant dust condensation. However, ONe nova eruptions tend to produce mainly O-rich dust, especially silicates (Gehrz et al. 1998; José et al. 2004). Although novae are more frequent ($35 \pm 11 \text{ yr}^{-1}$) than supernova explosions ($\sim 0.02 \text{ yr}^{-1}$), they contribute only 0.1% of the Galactic interstellar dust (Shafter 1997; Gehrz et al. 1998).

We report the isotopic and major element composition for one unusual presolar silicate grain from the CR chondrite Graves Nunataks (GRA) 95229. Measurement of several isotope systems (O, Mg, Si) allows us to constrain its stellar source to a classical nova outburst. Several presolar silicates and oxides of likely nova origin have been reported to date (Nittler et al. 1997, 2008, 2012; Choi et al. 1999; Nguyen et al. 2003, 2007, 2010a, 2010b, 2011a, 2011b; Vollmer et al. 2007; Gyngard et al. 2009, 2010, 2011; Bose et al. 2010), but the grain of this study is the first specimen with a significant ^{30}Si -excess. Preliminary results have been reported by Leitner et al. (2012).

⁴ Author to whom correspondence should be addressed.

Table 1
Oxygen, Magnesium, and Silicon Isotopic Compositions of Nova Candidate Silicates and Oxides

Grain	Ref. ^a	$^{17}\text{O}/^{16}\text{O}$ ($\times 10^{-4}$)	$^{18}\text{O}/^{16}\text{O}$ ($\times 10^{-3}$)	$\delta^{25}\text{Mg}$ (‰)	$\delta^{26}\text{Mg}$ (‰)	$\delta^{29}\text{Si}$ (‰)	$\delta^{30}\text{Si}$ (‰)
Presolar silicate grains							
GR95_13_29	This work	62.54 ± 2.51	1.96 ± 0.14	79 ± 21	70 ± 20	-16 ± 63	379 ± 92
4_7	N10a	149	1.29	215 ± 57	19 ± 48	~0	~0
B2-7	B10	133 ± 1	1.43 ± 0.04	±	±	21 ± 56	57 ± 69
4_2	N11a,b	128	1.75	1025	90	~0	~0
A094_TS6	N07	95.35 ± 1.14	1.50 ± 0.01			29 ± 43	43 ± 54
AH-106a	N10b	50.1 ± 2.16	1.78 ± 0.07			15 ± 59	80 ± 67
1_06	V07	49.1 ± 3.60	1.36 ± 0.19				
Presolar oxide grains							
C4-8	G10	440.4 ± 1.23	1.10 ± 0.02	949 ± 8	929 ± 8		
T 54	Ni97	141 ± 5	0.5 ± 0.02				
12-20-10	G10	88.01 ± 2.97	1.18 ± 1.10				
KC33	Ni08	82.2 ± 0.6	0.68 ± 0.08				
S-C6087	Ch99	75.2 ± 0.25	2.18 ± 0.025	36 ± 22	36 ± 22		
MCG68	N03	62.6 ± 1.08	1.89 ± 0.02				
KC23	Ni08	58.5 ± 1.80	2.19 ± 0.06	45 ± 35	5 ± 35		
8-9-3	G10	51.4 ± 1.05	1.89 ± 0.07	-66 ± 21	25 ± 21		
MCG67	N03	47.3 ± 1.42	1.77 ± 0.03				
Solar system		3.83	2.01	0	0	0	0

^a **References.** B10: Bose et al. 2010; Ch99: Choi et al. 1999; G09, G10: Gyngard et al. 2009, 2010; N03, N07, N10a&b, N11a&b: Nguyen et al. 2003, 2007, 2010a, 2010b, 2011a, 2011b; Ni97, Ni08: Nittler et al. 1997, 2008; V07: Vollmer et al. 2007.

2. EXPERIMENTAL

Grain GR95_13_29 was discovered in thin section 97 from the Antarctic CR2 chondrite GRA 95229 (obtained from the Johnson Space Center Meteorite Curation Facility) by semi-automated (“chained analysis”) ion imaging with the NanoSIMS 50 at the Max Planck Institute for Chemistry. For initial O-isotopic measurements, a Cs⁺ primary beam (100 nm diameter, ~1 pA) was rastered over 10 × 10 μm² sized sample areas (256 × 256 pixels). The total integration time for each field was ~55 minutes. Secondary ion (SI) images of ^{16,17,18}O⁻, ²⁸Si⁻, and ²⁷Al¹⁶O⁻ were acquired in multi-collection mode. Prior to analysis, sample areas of 14 × 14 μm² were presputtered with a high-current primary beam (~20 pA) to remove the carbon coating on selected regions. After realocalization and high-resolution imaging with a LEO 1530 FE-SEM, the elemental composition of GR95_13_29 was analyzed with the PHI 700 Auger Nanoprobe at Washington University in St. Louis, MO, using established procedures for presolar silicate grains (Stadermann et al. 2009); details are given by Floss & Stadermann (2009).

The Si-isotopic composition of the grain was measured again with the Cs⁺ primary source by scanning over a field of view of 3 × 3 μm² (128 × 128 pixels, ~80 minutes integration time). ^{28,29,30}Si⁻ were measured in multi-collection mode, together with ^{16,17}O⁻ for grain identification. To minimize contribution from surrounding matrix grains during Mg isotope analysis, the grain was isolated following the focused ion beam (FIB) procedure described in Nguyen et al. (2010a) and Kodolányi & Hoppe (2010, 2011) with a FEI Helios 600 instrument at the University of Saarland (Saarbrücken, Germany). After preparation, a 6 × 6 μm² area (256 × 256 pixels) including the grain was scanned with an ~80 nm primary Cs⁺ beam, while ¹²C⁻, ^{16,17,18}O⁻, and ²⁸Si⁻ were recorded to monitor the destruction of the protective C-cap deposited during FIB-preparation. As soon as the grain was identified by its ¹⁷O/¹⁶O

ratio, the scanning was stopped. For the Mg isotope analysis, a 200–250 nm O⁻ primary beam (~1 pA) was rastered over the same field of view, and ^{24,25,26}Mg⁺ as well as ²⁷Al⁺ were measured simultaneously.

3. RESULTS AND DISCUSSION

Results of the isotopic measurements are listed in Table 1, together with O-, Mg-, and Si-isotopic data of presolar nova candidate silicates and oxides from the literature. Isotopic compositions are reported either as isotopic ratios or as δ -values (deviation of a measured ratio of isotopes R_i and R_j from solar system composition in per mil ($\delta R_i = [(R_i/R_j)/(R_i/R_j)_{\text{standard}} - 1] \times 1000$)).

GR95_13_29 has an O-isotopic composition of $^{17}\text{O}/^{16}\text{O} = (6.25 \pm 0.25) \times 10^{-3}$ and $^{18}\text{O}/^{16}\text{O} = (1.96 \pm 0.14) \times 10^{-3}$ (Figure 1). The grain has about solar $^{29}\text{Si}/^{28}\text{Si}$ ($\delta^{29}\text{Si} = -16 \pm 63\text{‰}$) and is significantly enriched in ^{30}Si ($\delta^{30}\text{Si} = 379 \pm 92\text{‰}$; Figure 3). The Mg-isotopic composition was determined to be $\delta^{25}\text{Mg} = 79 \pm 21\text{‰}$ and $\delta^{26}\text{Mg} = 70 \pm 20\text{‰}$ (Figure 4). Contributions from surrounding matrix material to the Mg and Si isotopic compositions could not be eliminated completely, and the values reported for GR95_13_29 in Table 1 should be considered as lower limits.

From the high-resolution SEM image (Figure 2(a)), a compound/polygrain structure of the grain is clearly visible (the dotted line in each panel corresponds to the outline of the ¹⁷O-anomaly). Element distribution maps of Mg, Si, S, and Fe for GR95_13_29 and the surrounding matrix are shown in Figures 2(b)–(e). Neither Al nor Ca above detection limit is present. All detected elements show a heterogeneous distribution within the grain; two subareas with high Si contents (Figure 2(c)) are surrounded by material with lower Si and higher Mg abundances (Figure 2(b)). Sulfur is present in three

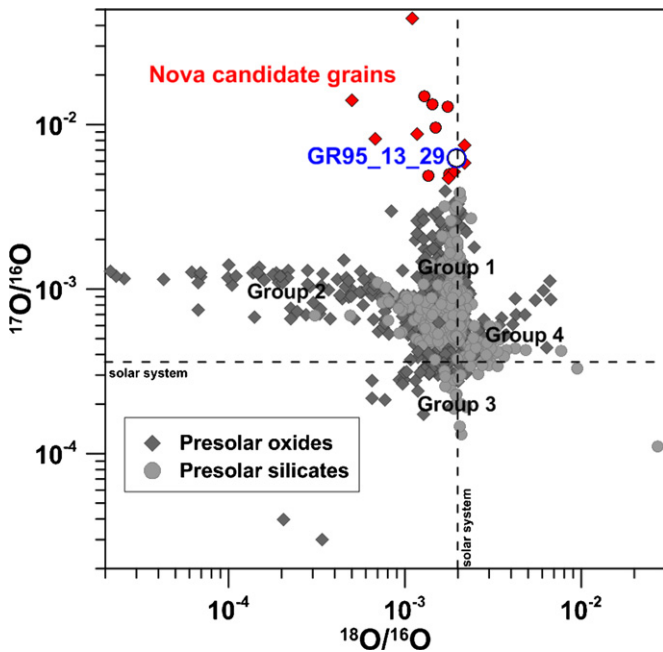


Figure 1. Three-isotope plot for oxygen showing presolar silicate and oxide grains discovered to date (Hynes & Gyngard 2009). Potential nova grains are marked by the red symbols (for references, see Table 1), together with GR95_13_29 from this study (white circle). Additionally, solar system isotopic composition is represented by the dashed lines.

(A color version of this figure is available in the online journal.)

distinct areas (Figure 2(d)), roughly correlated with elevated Fe abundances (Figure 2(e)).

Quantitative results were obtained for two spots (denoted by “1” and “2” in Figure 2(a)); the element abundances are O = 55 at%, Mg = 11 at%, Si = 17 at%, S = 3 at%, Fe = 14 at% (region 1), and O = 61 at%, Mg = 8 at%, Si = 22 at%, and Fe = 9 at% (region 2). Relative abundance errors, based on relative uncertainties in the sensitivity factors from standard measurements (Stadermann et al. 2009), are 3.6% for O, 9.4% for Mg, 11% for Si, 10% for S, and 11.2% for Fe, respectively. No background correction was applied, and the measurement was affected by charging, so that the true uncertainties have to be assumed larger than the ones reported above. We calculate Mg/Si ratios of 0.66 ± 0.09 (region 1) and 0.34 ± 0.05 (region 2), as well as Fe/Si ratios of 0.66 ± 0.12 (region 1) and $0.39 \pm$

0.06 (region 2), respectively. The Fe abundance for the silicate fraction was corrected by assuming that S is present in the form of FeS; the uncorrected Fe/Si- and (Mg + Fe)/Si-values for region 2 are slightly higher. (Mg + Fe)/Si is 1.3 ± 0.2 for region 1, characteristic for the “intermediate” type of presolar silicates with a stoichiometry between olivine and pyroxene, and region 2 displays (Mg + Fe)/Si = 0.7 ± 0.1 , indicating a Si-rich silicate (e.g., Floss & Stadermann 2009).

The $^{17}\text{O}/^{16}\text{O}$ ratios of red giant and AGB star grains are sensitive measures for the mass of the parent stars. Their O-isotopic compositions are mostly determined by the first dredge-up, when matter that experienced H-burning by the CNO cycle is brought to the surface. The first dredge-up leads to enhanced $^{17}\text{O}/^{16}\text{O}$ ratios in the stellar envelope, with the highest ratios predicted for $2\text{--}3 M_{\odot}$ stars (Boothroyd & Sackmann 1999; Cristallo et al 2009). The $^{18}\text{O}/^{16}\text{O}$ ratio is much less affected by the first dredge-up, and grains from stars with $M < 4 M_{\odot}$ that did not experience cool bottom processing will have $^{18}\text{O}/^{16}\text{O}$ ratios only slightly lower than the initial ratio at stellar birth. For heavier stars hot bottom burning (HBB; Boothroyd et al. 1995; Lugaro et al. 2007) is likely to occur which will destroy essentially all ^{18}O . The $^{18}\text{O}/^{16}\text{O}$ ratio of grain GR95_13_29 of $(1.96 \pm 0.14) \times 10^{-3}$ implies a progenitor star of \sim solar or slightly higher than solar metallicity ($Z_{\odot} = 0.014$; Asplund et al. 2009) with relatively low mass ($1\text{--}1.5 M_{\odot}$). The maximum $^{17}\text{O}/^{16}\text{O}$ ratio that can be produced in such single AGB stars is $\sim 1 \times 10^{-3}$ (Cristallo et al. 2009; Palmerini et al. 2011), lower than the value observed for GR95_13_29. Stars with $M = 2\text{--}3 M_{\odot}$ and $Z = 0.5\text{--}1 Z_{\odot}$ reach $^{17}\text{O}/^{16}\text{O}$ ratios of $4\text{--}6 \times 10^{-3}$, close to the value of GR95_13_29. However, in this case predicted $^{18}\text{O}/^{16}\text{O}$ ratios would be too low by about 25% compared to GR95_13_29. Further evidence against an AGB star origin of grain GR95_13_29 comes from its Si isotopes. Its Si-isotopic composition lies in the range observed for the rare (a few percent) SiC grains of type Z. The parent stars of these grains are AGB stars of subsolar metallicity ($Z \sim \frac{1}{3} Z_{\odot}$) (Hoppe et al. 1997; Amari et al. 2001; Zinner et al. 2006). Zinner et al. (2006) investigated in detail two different sets of stellar evolution models (FRANEC- and MONASH-code) to identify the stellar origins of Z grains. Significant ^{30}Si -enrichments occur, according to these models, generally during third dredge-up events, when products of partial He-burning and neutron capture nucleosynthesis are mixed to the stellar surface. This material consists mainly of ^{12}C from the

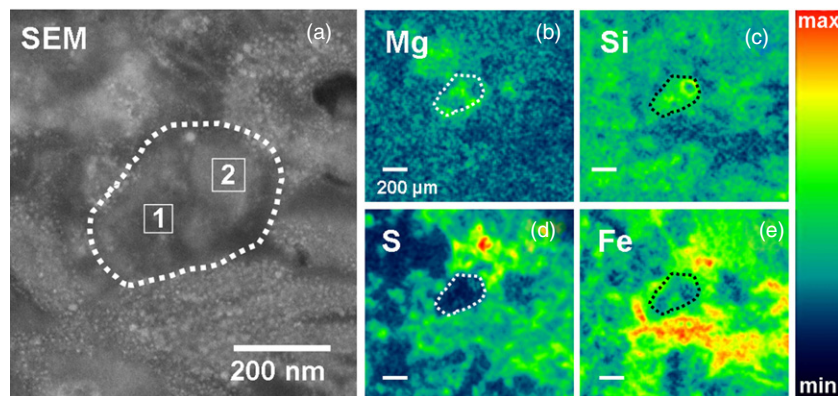


Figure 2. (a) SEM and (b) Auger electron spectroscopy element maps of magnesium, (c) silicon, (d) sulfur, and (e) iron. The color scale bar indicates element signal intensities for panels (b)–(e). All scale bars are 200 nm; the outline of the grain is highlighted in each panel by a dotted line. The numbers “1” and “2” in panel (a) denote the spots from which quantitative data were obtained.

(A color version of this figure is available in the online journal.)

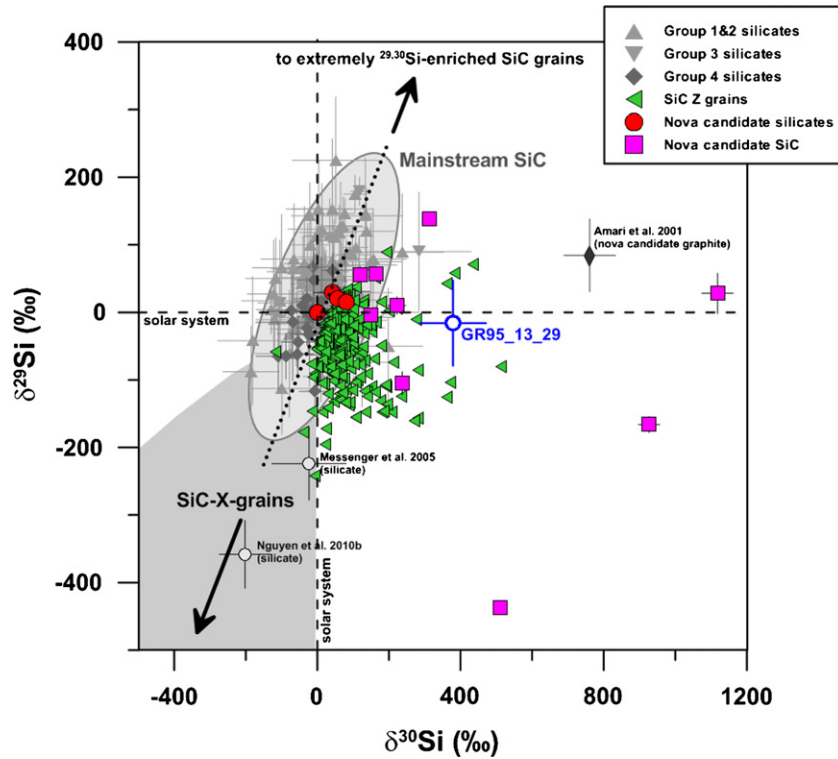


Figure 3. Three-isotope plot for silicon. Solar system composition is denoted by the dashed lines. The data for the reference nova candidate silicates are listed in Table 1; data for SiC Z, nova candidate SiC, and Group 1–4 presolar silicate grains are taken from Hynes & Gyngard (2009). The range of Si-isotopic compositions for mainstream SiC is marked by the gray ellipse, and the dotted line denotes the SiC mainstream line (Zinner et al. 2006). (A color version of this figure is available in the online journal.)

He-burning process, resulting in $C/O > 1$ in the envelope and turning the star into a carbon star. This precludes condensation of O-rich dust during this episode of stellar evolution, since all oxygen is bound in the very stable CO molecule (Lodders & Fegley 1995). Potential ^{30}Si -rich silicates must be produced before the third dredge-up raises C/O above unity. Only the $M = 5 M_{\odot}$ star model with $Z = 0.004$ from the MONASH code yields a significant ^{30}Si excess ($\delta^{30}\text{Si} = 854\text{‰}$) at $C/O = 1$ (Zinner et al. 2006). Stars with $M > 4 M_{\odot}$ are likely to experience HBB which leads to $^{18}\text{O}/^{16}\text{O}$ ratios orders of magnitude lower than the nearly solar value observed for grain GR95_13_29. Therefore, we can exclude an AGB star origin for GR95_13_29.

We explored the SNI models by Rauscher et al. (2002)⁵ to investigate a possible core-collapse supernova origin. No single zone in any of the models can reproduce the isotopic compositions; the same holds true for mixing of multiple zones. The highest $^{17}\text{O}/^{16}\text{O}$ ratios are predicted for the He/N zone with ^{17}O enrichments of factors of 4 ($15 M_{\odot}$ SNI) and 5 ($25 M_{\odot}$ SNI), clearly lower than the enrichment of a factor of 16 observed for grain GR95_13_29. Moreover, a ^{30}Si excess requires material from the O/Si or O/C zones (where $^{17}\text{O}/^{16}\text{O}$ is significantly lower than solar), and admixture of matter from these zones would further lower $^{17}\text{O}/^{16}\text{O}$ ratios drastically.

Type Ia supernovae are caused by the thermonuclear explosion of a mass-accreting white dwarf in a binary system (e.g., Nomoto et al. 1997, and references therein), resulting in the total disruption of the white dwarf. Hydrodynamic calculations yield subsolar O-isotopic ratios ($2.3 \times 10^{-9} \leq ^{17}\text{O}/^{16}\text{O} \leq 6.1 \times 10^{-5}$ and $1.8 \times 10^{-9} \leq ^{18}\text{O}/^{16}\text{O} \leq 6.2 \times 10^{-6}$, respectively), as well as enrichments in ^{24}Mg and ^{28}Si . Recently, Li et al. (2011)

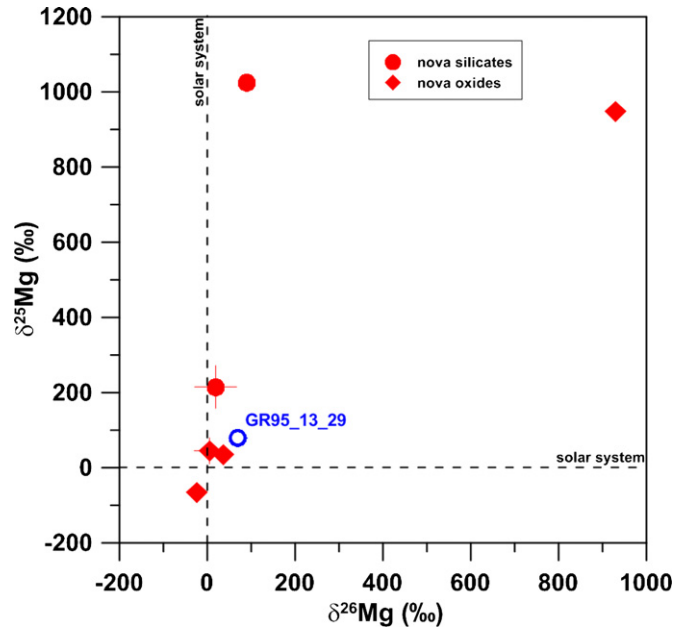


Figure 4. Three-isotope plot for magnesium. Solar system composition is denoted by the dashed lines. The data for the reference nova candidate grains are listed in Table 1. (A color version of this figure is available in the online journal.)

identified the merger of two white dwarfs as the most probable scenario for SN 2011fe. Compared to the data from Nomoto et al. (1997), such a scenario would result in even more extreme enrichments in ^{16}O , ^{24}Mg , and ^{28}Si . Thus, we can rule out an SN origin for this grain.

⁵ <http://www.nucleosynthesis.org>

We noted before that the maximum $^{17}\text{O}/^{16}\text{O}$ ratio that can be achieved by single AGB star nucleosynthesis is $\sim 6 \times 10^{-3}$ for $Z = 0.5\text{--}1.5 Z_{\odot}$. A possible scenario to circumvent this “single AGB cutoff” barrier is by mass transfer in close binary star systems, when one component is “polluted” with material from the other star (Marks et al. 1997). This mechanism has been invoked to explain extreme $^{17}\text{O}/^{16}\text{O}$ ratios as well as unusually high ^{25}Mg and ^{26}Mg excesses observed in some presolar grains (Nittler et al. 2008). Type Ia supernovae, which are stricto sensu also mass-transferring binaries, have been discussed previously, and nova outbursts will be treated below. Based on the conclusions derived for single AGB stars let us first consider a binary system consisting of a low-mass main-sequence star ($1\text{--}1.5 M_{\odot}$) and an intermediate-mass AGB star ($5 M_{\odot}$). We assume that both stars have the same metallicity, namely lower than solar, to account for the observed ^{30}Si enrichments. When a star expands beyond its Roche lobe (i.e., the region in which the stellar material is gravitationally bound to its host), matter from the envelope is transferred through the inner Lagrangian point of the binary system to the companion star. The heavier component of the system transfers material enriched in ^{17}O and ^{30}Si to the companion star. Increased ^{17}O abundance and the later first dredge-up in the companion star can easily raise the $^{17}\text{O}/^{16}\text{O}$ ratio to a level observed in GR95_13_29. For $M = 5 M_{\odot}$ and $Z = 0.004$, the final $\delta^{30}\text{Si}$ is predicted to be $\sim 1000\%$ at $\text{C}/\text{O} \sim 2$ (Zinner et al. 2006). Before mass transfer, the low-mass companion star will have its initial Si-isotopic composition, assumed to be $\delta^{30}\text{Si} = -150\%$ (Zinner et al. 2006), and $\text{C}/\text{O} = 0.5$. Mixing matter from the mass-losing star with the envelope of the low-mass companion star in a ratio 1:1 results in $\delta^{30}\text{Si} \sim 400\%$, as observed in GR95_13_29, and C/O not far from unity. However, because HBB leads to a very low $^{18}\text{O}/^{16}\text{O}$ ratio in the envelope of the mass-losing star, this mass transfer will lower the $^{18}\text{O}/^{16}\text{O}$ ratio in the envelope of the companion star, which is already assumed to be lower than solar (Cristallo et al. 2009), by about a factor of two, inconsistent with the data for GR95_13_29. We thus exclude an origin from a binary system consisting of a low-mass main-sequence/red giant star and an intermediate-mass AGB star as source of grain GR95_13_29.

Classical novae are predicted to produce large enrichments in ^{13}C , ^{15}N , and ^{17}O and $^{17}\text{O}/^{16}\text{O}$ ratios $> 6 \times 10^{-3}$; the models predict higher ratios for ONe than for CO novae. ^{18}O is strongly depleted in CO novae, while ONe models yield a wide range of ratios, due to the higher peak temperatures (and the resulting synthesis of larger amounts of $^{17,18}\text{O}$).

Both nova types yield $^{25}\text{Mg}/^{24}\text{Mg}$ and $^{26}\text{Mg}/^{24}\text{Mg}$ ratios of $\sim 3.3\text{--}50$ and $\sim 0.23\text{--}10$, respectively (José et al. 2004). For CO novae, Mg synthesis depends strongly on the attained maximum temperature and the initial Mg abundances, while this is not the case for ONe novae. For the latter, a significant decrease of ^{24}Mg and ^{26}Mg is observed, which results in higher than solar $^{25}\text{Mg}/^{24}\text{Mg}$ ratios. Synthesis of ^{26}Al depends strongly on the peak temperatures, as well as the time spent at these temperatures. Nittler & Hoppe (2005) pointed out that the $^{26}\text{Al}/^{27}\text{Al}$ ratios of novae and supernovae have similar ranges and cannot be used to constrain the stellar sources of presolar grains.

CO novae display only very limited nucleosynthetic activity beyond the mass region of the CNO elements. The maximum temperatures during the explosion and the absence of significant amounts of seed nuclei forestall the production of Si isotopes, and solar-like Si-ratios are predicted by the models. ONe novae, in contrast, attain higher peak temperatures and contain sufficient heavier nuclei for the synthesis of silicon isotopes.

The ^{28}Si abundances increase from the 1 to $1.25 M_{\odot}$ models and drop slightly for higher masses (José et al. 2004), where the p -capture destruction of ^{28}Si dominates all synthesis reactions. The abundances of ^{29}Si and ^{30}Si increase monotonically with M_{WD} , and ^{30}Si -excesses are predicted for $M_{\text{WD}} \geq 1.25 M_{\odot}$. The $^{29}\text{Si}/^{28}\text{Si}$ ratios are below solar and reach \sim solar system values for $M_{\text{WD}} \sim 1.35 M_{\odot}$ (José et al. 2004).

We explored the ONe models from José & Hernanz (1998) and focused on the models ONe3 ($1.15 M_{\odot}$ with 50% ad hoc-mixing), ONe5 ($1.25 M_{\odot}$ with 50% ad hoc-mixing), and ONe6 ($1.35 M_{\odot}$ with 50% ad hoc-mixing). For these three scenarios, the O-isotopic compositions were modified according to Gyngard et al. (2011). For the ONe6 model, we observe a good match with the isotopic composition of GR95_13_29 if we assume a nova contribution of $\sim 1\%$ to material from a companion star of solar composition. We find $^{17}\text{O}/^{16}\text{O} = (6.0\text{--}6.6) \times 10^{-3}$, $^{18}\text{O}/^{16}\text{O} \sim 2 \times 10^{-3}$, $\delta^{25}\text{Mg} = (59\text{--}66)\%$, $\delta^{26}\text{Mg} = (16\text{--}18)\%$ (with ^{26}Al -contribution), $\delta^{29}\text{Si} = 2\%$, and $\delta^{30}\text{Si} = (450\text{--}494)\%$.

An aggregate- or polygrain-like structure could be a qualitative indicator in ejecta of SNII ejecta, in contrast to single crystals which are more likely to be formed around red giant/AGB stars (Vollmer et al. 2008, references therein). GR95_13_29, albeit not likely an SN condensate, displays a comparable structure; this fact supports the idea of grain formation in an explosive scenario like a nova eruption. The presence of a Si-rich subgrain with $(\text{Mg} + \text{Fe})/\text{Si}$ lower than what is characteristic for pyroxene-like materials (~ 1) is also characteristic for condensation under non-equilibrium conditions (Nagahara & Ozawa 2008).

4. CONCLUSIONS

The oxygen, magnesium, and silicon isotopic compositions of GR95_13_29 indicate an origin of this presolar silicate grain in the ejecta of a $1.35 M_{\odot}$ ONe nova mixed with 99.9% of material of solar composition from the companion star. The morphology and elemental composition determined by SEM and Auger Electron Spectroscopy support condensation under non-equilibrium conditions as observed for dust shells of nova eruptions. A full quantitative modeling of the grain data is currently not feasible, due to the uncertainties of the reaction rates used in novae nucleosynthesis models, and to the new developments in nova modeling, especially first three-dimensional computations (e.g., Casanova et al. 2011). However, we are able to exclude other stellar origins for GR95_13_29, and find good agreement between the presolar grain isotopic data and a specific ONe nova model.

We thank Elmar Gröner for technical support on the NanoSIMS, Joachim Huth for assistance with the SEM, Christoph Pauly for FIB-preparation, Frank Gyngard for helpful discussions on nova mixing calculations, and an anonymous reviewer for constructive comments. SN models from www.nucleosynthesis.org were provided by Alexander Heger. J.L. and P.H. acknowledge support by DFG through SPP 1385. The work at Washington University in St. Louis is funded by NASA grant NNX10AH43G (C.F.).

REFERENCES

- Amari, S., Nittler, L. R., Zinner, E., et al. 2001, *ApJ*, **546**, 248
 Asplund, M., Grevesse, N., Sauval, A. J., & Scott, P. 2009, *ARA&A*, **47**, 481

- Boothroyd, A. I., Sackmann, I.-J., & Wasserburg, G. J. 1995, *ApJ*, **442**, L21
- Boothroyd, A. I., & Sackmann, I.-J. 1999, *ApJ*, **510**, 232
- Bose, M., Zhao, X., Floss, C., Stadermann, F. J., & Lin, Y. 2010, in Proc. 11th Symp. on Nuclei in the Cosmos, 2010 July 19–23, Heidelberg, Germany, available online at http://pos.sissa.it/archive/conferences/100/138/NIC%20XI_138.pdf
- Casanova, J., José, J., García-Berro, E., Shore, S. N., & Calder, A. C. 2011, *Nature*, **478**, 490
- Choi, B.-G., Wasserburg, G. J., & Huss, G. R. 1999, *ApJ*, **522**, L33
- Cristallo, S., Straniero, O., Gallino, R., et al. 2009, *ApJ*, **696**, 797
- Floss, C., & Stadermann, F. J. 2009, *Geochim. Cosmochim. Acta*, **73**, 2415
- Gehrz, R. D., Truran, J. W., Williams, R. E., & Starrfield, S. 1998, *PASP*, **110**, 3
- Gyngard, F., Morgand, A., Nittler, L. R., Stadermann, F. J., & Zinner, E. 2009, *Lunar Planet. Sci. Conf.*, **40**, 1386
- Gyngard, F., Nittler, L. R., Zinner, E., José, J., & Cristallo, S. 2011, *Lunar Planet. Sci. Conf.*, **42**, 2675
- Gyngard, F., Zinner, E., Nittler, L. R., et al. 2010, *ApJ*, **717**, 107
- Hoppe, P. 2008, *Space Sci. Rev.*, **138**, 43
- Hoppe, P., Annen, P., Strebler, R., et al. 1997, *ApJ*, **487**, L101
- Hynes, K. M., & Gyngard, F. 2009, *Lunar Planet. Sci. Conf.*, **40**, 1198
- José, J., & Hernanz, M. 1998, *ApJ*, **494**, 680
- José, J., Hernanz, M., Amari, S., Lodders, K., & Zinner, E. 2004, *ApJ*, **612**, 414
- Kodolányi, J., & Hoppe, P. 2010, in Proc. 11th Symp. on Nuclei in the Cosmos, 2010 July 19–23, Heidelberg, Germany, available online at http://pos.sissa.it/archive/conferences/100/142/NIC%20XI_142.pdf
- Kodolányi, J., & Hoppe, P. 2011, *Lunar Planet. Sci. Conf.*, **42**, 1094
- Leitner, J., Hoppe, P., & Zipfel, J. 2012, *Lunar Planet. Sci. Conf.*, **43**, 1835
- Li, W., Bloom, J. S., Podsiadlowski, P., et al. 2011, *Nature*, **480**, 348
- Lodders, K., & Fegley, B., Jr. 1995, *Meteoritics*, **30**, 661
- Lugaro, M., Karakas, A. I., Nittler, L. R., et al. 2007, *A&A*, **461**, 657
- Marks, P. B., Sarna, M. J., & Prialnik, D. 1997, *MNRAS*, **290**, 283
- Nagahara, H., & Ozawa, K. 2008, *Lunar Planet. Sci. Conf.*, **39**, 1241
- Nguyen, A. N., Keller, L. P., Rahman, Z., & Messenger, S. 2011a, *Meteor. Planet. Sci.*, **46**, A177
- Nguyen, A. N., Messenger, S., Ito, M., & Rahman, Z. 2010a, *Lunar Planet. Sci. Conf.*, **41**, 2413
- Nguyen, A. N., Messenger, S., Ito, M., & Rahman, Z. 2011b, *Lunar Planet. Sci. Conf.*, **42**, 2711
- Nguyen, A. N., Nittler, L. R., Stadermann, F. J., Stroud, R. M., & Alexander, C. M. O'D. 2010b, *ApJ*, **719**, 166
- Nguyen, A. N., Stadermann, F. J., Zinner, E., et al. 2007, *ApJ*, **656**, 1223
- Nguyen, A. N., Zinner, E., & Lewis, R. S. 2003, *PASA*, **20**, 382
- Nittler, L. R., Alexander, C. M. O'D., Gallino, R., et al. 2008, *ApJ*, **682**, 1450
- Nittler, L. R., Alexander, C. M. O'D., Gao, X., Walker, R. M., & Zinner, E. 1997, *ApJ*, **483**, 475
- Nittler, L. R., & Hoppe, P. 2005, *ApJ*, **631**, L89
- Nittler, L. R., Wang, J., & Alexander, C. M. O'D. 2012, *Lunar Planet. Sci. Conf.*, **43**, 2442
- Nomoto, K., Iwamoto, K., Nakasato, N., et al. 1997, *Nucl. Phys. A*, **621**, 467c
- Palmerini, S., La Cognata, M., Cristallo, S., & Busso, M. 2011, *ApJ*, **729**, 3
- Rauscher, T., Heger, A., Hoffman, R. D., & Woosley, S. E. 2002, *ApJ*, **576**, 323
- Shafter, A. W. 1997, *ApJ*, **487**, 226
- Shore, S. N., Starrfield, S., González-Riestra, R., Hauschildt, P. H., & Sonneborn, G. 1994, *Nature*, **369**, 539
- Stadermann, F. J., Floss, C., Bose, M., & Lea, A. S. 2009, *Meteor. Planet. Sci.*, **44**, 1033
- Vollmer, C., Hoppe, P., & Brenker, F. E. 2008, *ApJ*, **684**, 611
- Vollmer, C., Hoppe, P., Brenker, F. E., & Holzappel, C. 2007, *ApJ*, **666**, L49
- Zinner, E. 2007, in *Treatise on Geochemistry*, Vol. 1: Meteorites, Comets, and Planets, Presolar Grains, ed. A. M. Davis (Amsterdam: Elsevier), 1
- Zinner, E., Nittler, L. R., Gallino, R., et al. 2006, *ApJ*, **650**, 350